

Dynamic evaluation of composite roofs: thermal optimization with PCM under extreme climate conditions

Evaluación dinámica de techos compuestos: optimización térmica mediante PCM en condiciones climáticas extremas

López Salazar, Samanta ^a, Simá, E. ^b, Chagolla-Aranda, M. A. ^c and Chávez-Chena, Y. ^d

^a TecNM/CENIDET • LBH-6330-2024 • 0009-0004-9880-5145 • 918135

^b TecNM/CENIDET • JZS-9886-2024 • 0000-0001-7601-1273 • 83891

^c TecNM/CENIDET • LBI-3033-2024 • 0000-0002-7649-7389 • 368646

^d TecNM/CENIDET • LBH-6345-2024 • 0000-0003-3348-397X • 37563

CONAHCYT classification:

Area: Engineering

Field: Engineering

Discipline: Mechanical Engineering

Subdiscipline: Thermal Engineering

<https://doi.org/10.35429/JCE.2024.8.19.1.14>

Article History:

Received: January 25, 2024

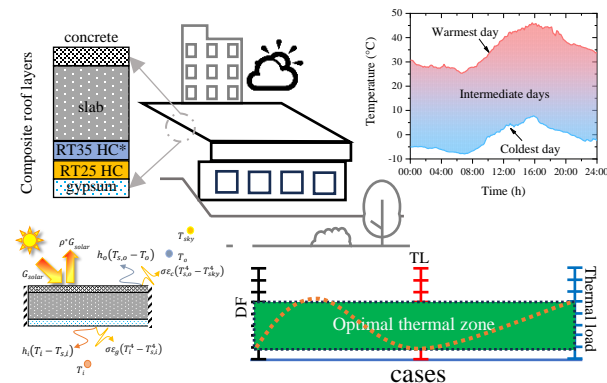
Accepted: December 31, 2024

* [\[d18ce057@cenidet.tecnm.mx\]](mailto:d18ce057@cenidet.tecnm.mx)



Abstract

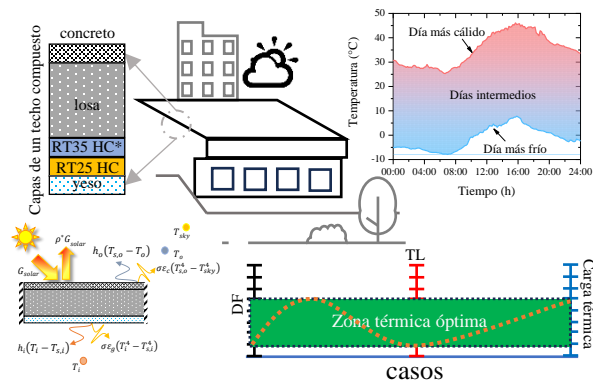
The thermal performance of different roof configurations was analyzed, comparing the integration of phase change materials (PCM) with polystyrene insulation under extreme climatic conditions. The decrement factor (DF), time lag (TL), and thermal load were examined. The results indicated that configuration with PCM, either in double layers or with increased thickness, showed the best thermal performance. The optimal configuration, C45, which includes a double layer of PCM with RT25 HC on the bottom layer and RT35 HC* at the top layer, achieved a DF of less than 0.2, a TL between 2 and 10 hours, and a thermal load of 2.5 kWhm⁻². This study confirms that adding a PCM layer is the most effective strategy, followed by the increase of the thickness, as well as the addition of insulation, and finally, an additional layer.



Composite roofs, Thermal insulation, Beat management

Resumen

Se analizó el rendimiento térmico de diferentes configuraciones de techos, comparando la integración de materiales de cambio de fase (PCM) con el aislamiento de poliestireno en condiciones climáticas extremas. Se analizó el factor de decremento (DF), el tiempo de retardo (TL) y la carga térmica. Los resultados indicaron que las configuraciones con PCM, ya sea en doble capa o con mayor espesor, presentaron el mejor rendimiento térmico. La configuración óptima, C45, que incluye una doble capa de PCM con RT25 HC en la capa inferior y RT35 HC* en la capa superior, logró un DF inferior a 0.2, un TL entre 2 y 10 h, y una carga térmica 2.5 kWhm⁻². Este estudio confirma que añadir una capa de PCM es la estrategia más efectiva, seguida por el incremento del espesor, agregar aislamiento y, por último, una capa adicional.



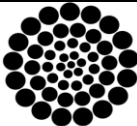
Techo compuesto, Aislamiento térmico, Gestión de calor

Citation: López Salazar, Samanta, Simá, E., Chagolla-Aranda, M. A. and Chávez-Chena, Y. [2024]. Dynamic evaluation of composite roofs: thermal optimization with PCM under extreme climate conditions. Journal Civil Engineering. 8[19]-1-14: e30819114.



ISSN 2523-2428/© 2009 The Author[s]. Published by ECONFAN-Mexico, S.C. for its Holding Republic of Peru on behalf of Journal Civil Engineering. This is an open access article under the CC BY-NC-ND license [<http://creativecommons.org/licenses/by-nc-nd/4.0/>]

Peer Review under the responsibility of the Scientific Committee MARVID® - in contribution to the scientific, technological and innovation Peer Review Process by training Human Resources for the continuity in the Critical Analysis of International Research.



RENIECYT
Registro Nacional de Instituciones y
Empresas Científicas y Tecnológicas

1702902

CONAHCYT

Introduction

As global temperatures rise due to climate change, the residential sector faces increasing demand for electricity, particularly to maintain thermal comfort. Worldwide, buildings are responsible for about 40.0 % of total energy consumption and contribute roughly 33.0 % of global greenhouse gas emissions. Heating and cooling systems, which are important for maintaining indoor climate control, account for 50.0 % to 70.0 % of a building's total energy use, depending on the climate and the efficiency of the building envelope (Somu et al., 2021). The increased use of these systems, driven by higher temperatures, has intensified this demand, putting additional strain on energy resources (Mejía et al., 2020).

Thermal gain in a building, defined as the amount of unwanted heat entering through the building envelope, is a significant factor contributing to increased energy consumption. It is estimated that around 25.0 % of this thermal gain comes from windows, 35.0 % from walls, and approximately 30.0 % from roofs (Shove et al., 2014). These statistics emphasize the importance of thoughtful design and material selection to maximize energy efficiency, with a particular focus on roofs. Roofs play a crucial role in a building's thermal load due to their direct exposure to solar radiation and their larger surface area compared to other elements of the building envelope.

To mitigate these effects and reduce thermal gain in roofs, various construction solutions have been developed, such as ventilated roofs (Wang et al., 2024), reflective materials (Parikh et al., 2023), and thermal insulators (Shrimali & Agrawal, 2024). Among these, expanded polystyrene (EPS) is one of the most commonly used materials in construction due to the effectiveness in reducing heat transfer and the low cost. However, while EPS is effective at minimizing heat loss, the ability to dynamically manage thermal flow is limited compared to more advanced materials like phase change materials, PCM, (Arumugam et al., 2024).

In this context, PCM has emerged as an innovative solution for enhancing thermal management in construction, due to their capacity to absorb, store, and release large amounts of energy as latent heat during phase changes. This ability to more efficiently moderate indoor temperatures is particularly valuable in roofs, where direct exposure to solar radiation and temperature fluctuations can cause significant thermal variations inside the building.

Several studies have demonstrated the effectiveness of integrating PCM into roofs to reduce indoor thermal fluctuations and decrease the building's overall thermal load. Piselli et al. (2019) evaluated membranes with integrated PCM for roofs, finding that the inclusion of PCM lowered the roof's surface temperature and heat flow. Following this, Bhamare et al. (2020) developed a 3D model showing that a 2° inclination in the PCM layer provides optimal daily heat gain reduction and improves the melting and solidification cycle. Similarly, Arumugam & Shaik (2021) analyzed the thermo-economic performance of hollow roofs with PCM, finding that combining PCM in walls and roofs reduces air conditioning costs and CO₂ emissions. Moreover, Qu et al. (2021) evaluated four key parameters in building envelopes with PCM, concluding that the thickness and arrangement of PCM significantly influence energy efficiency, achieving energy savings of up to 34.8 %.

Following the findings of Bhamare et al. (2023), which demonstrated the effectiveness of PCM with a 2 cm air layer, Dardouri et al. (2023) conducted several studies evaluating the energy performance of buildings with PCM in Mediterranean climates. Using EnergyPlus, they discovered energy savings of up to 41.6 %, particularly with PCMs that have different melting temperatures. In another study, the same authors found that the optimal thickness of PCM and insulation layers can reduce energy demand by up to 76.5 % in double walls and 73.8 % in single walls (Dardouri et al., 2023). Additionally, further analysis of roofs and walls with PCM in various locations revealed that PCMs with melting temperatures of 21 °C are more effective for heating, while those with 29 °C optimize cooling savings (Dardouri et al., 2023).

In a separate study, Yu et al. (2023) conducted simulations to assess the effectiveness of PCM in reducing overheating in buildings during summer. The results showed a decrease in overheating hours between 10.9 % and 19.7 %, and a reduction in cooling energy consumption by between 14.6 % and 25.7 %.

Zahir et al. (2023) analyzed the use of thermal energy storage (TES) systems with PCM to enhance the thermal performance of buildings in extremely hot climates, identifying challenges in the selection and encapsulation of PCM due to small daytime temperature variations.

Meanwhile, Anter et al. (2023) evaluated the long-term thermal behavior of different PCM in walls, finding that RT-35HC, placed 1.5 cm from the interior and exterior of the wall, reduces the average internal temperature to 27.7°C and decreases energy gain by 66.0 % during summer.

Refahi et al. (2024) assessed the impact of a double layer of PCM boards with different melting points, achieving energy savings of 6.6 % in heating and 2.8 % in cooling. Moreover, Zhang et al. (2024) proposes an electric heating terminal with PCM thermal storage that improves thermal efficiency in Tibet and reduces melting time by 2.7 hours.

Finally, Khaleghi & Karatas (2024) assessed a prefabricated wall panel with PCM, which showed a decrement factor of 0.007 and a time lag of 8 hours under extreme weather. The panel showed superior thermal performance, enhancing energy efficiency and indoor comfort.

However, most of these studies have been conducted in regions where PCM use is regulated and widely accepted, unlike in Mexico, where conventional methods like expanded polystyrene are still the norm. While research has explored the integration of more complex PCM configurations, such as double layers with different melting points and strategic positioning within roof structures, these analyses have not yet been carried out in the Mexican context.

This study innovatively applies phase change materials (PCM) in composite roof configurations, exploring strategic combinations of different PCM types to optimize thermal efficiency in both extreme cold and hot weather conditions.

By incorporating double layers of PCM, the study not only improves thermal regulation across a wide temperature range but also maximizes heat storage capacity and thermal inertia. Furthermore, a detailed comparison with traditional extruded polystyrene highlights the superior performance of PCM in cold desert climates.

Focusing on a specific climate, such as that of Ciudad Juárez, adds regional relevance and practical value, demonstrating the model's applicability to areas with significant temperature fluctuations and underscoring the potential impact of these findings on sustainable construction practices.

Physical and mathematical model

Figure 1 shows the cross section of a 1.0 m long composite roof made out of several layers of materials. The reference configuration includes a 0.005 m thick external concrete layer, a 0.1 m thick of a reinforced concrete slab and a 0.005 m thick inside gypsum plaster layer.

This type of configuration is widely used in the residential and commercial construction sector, in particular in areas where a combination of structural durability together with an appropriate thermal efficiency is looked up.

This type of concrete slab is commonly found in family housing, office buildings and industrial warehouses, where the reinforced concrete slab provides the resistance needed to support loads, whereas the concrete and gypsum plaster layers act as added barriers helping to moderate the heat transfer.

The described roof configuration provides an equilibrium between construction costs and thermal performance, what make it a popular option for temperate and cold climates.

To optimize the thermal performance of this basic structure, this study incorporates additional layers on the inside surface as well as on the outside. These include a 0.025 m thick insulating polystyrene and phase change materials (PCM's) with different fusion temperatures and varying thickness (10 mm, 20 mm and 30 mm).

Besides, configurations with two layers of 10 mm thick PCM placed in different positions are evaluated. Figure 2 shows these configurations, and in total, the study covers 52 different variants, by alternating the locations of the single and double layers of the PCM as well as the thickness.

These configurations are submitted to a detailed analysis of the heat transfer process in order to evaluate the thermal performance under different environmental conditions.

Figure 3 shows the heat transfer processes experienced by the roof, which are exposed to environmental conditions (ambient temperature, solar radiation and wind velocity) through the upper boundary.

Due to the temperature difference, heat transfer by convection and radiation occurs on this surface, a similar phenomenon happens in the lower boundary that is kept at constant temperature.

One portion of the solar radiation hitting on the outside surface of the roof is absorbed by the concrete slab, provoking the temperature to increase, whereas other portion is reflected in the exterior environment.

The heat absorbed by the concrete slab increases the temperature, starting thus the heat transfer process by conduction throughout all the layers of the roof. This complex process of heat transfer is mathematically modeled in order to predict the behavior and efficiency.

Box 1

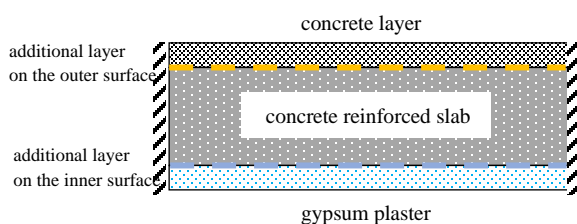


Figure 1

Cross section of a composite roof: reinforced concrete slab with concrete and gypsum plaster coats

Source: Own elaboration

Box 2

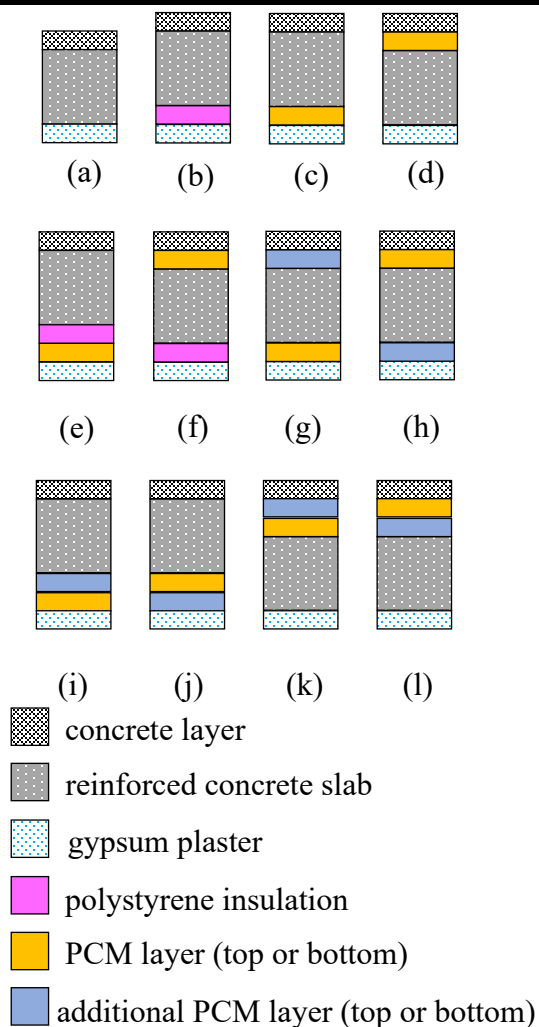


Figure 2

Configurations of the composite roof: layers material and location

Source: Own elaboration.

Box 3

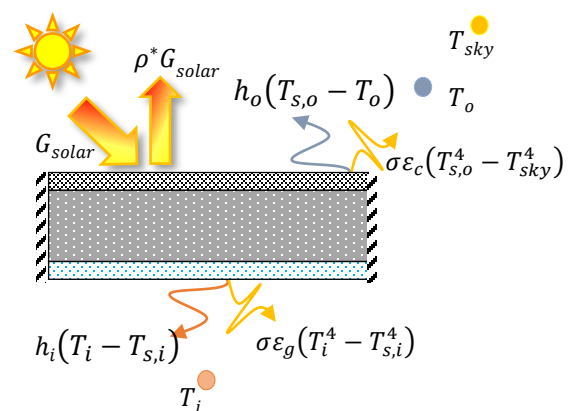


Figure 3

Heat transfer process on a composite roof subject to outside environmental conditions and at constant temperature on the inside surface

Source: Own elaboration.

The mathematical model describing the two-dimensional conduction heat transfer process is shown in Eq. (1). This equation applies to all the layers of the system (concrete, gypsum plaster, reinforced concrete and insulation), as well as the PCM, with the necessary adjustments to take into account the phase change. In order to perform such adjustments, the specific heat capacity method is used, and it introduces the term $C_{P\,eff}$, including the enthalpy term h_{ls} that occurs during the transition phase. This way, the effective heat capacity encompasses the energy storage as well as the latent heat associated with the phase change, as detailed in Eq. (2). In order to apply this model to a multilayer composite roof, it is important to take into account the way in which the different layer interact in the interfaces.

$$\frac{\partial(\rho C_P T)}{\partial t} = \frac{\partial}{\partial x} \left(\lambda \frac{\partial T}{\partial x} \right) + \frac{\partial}{\partial y} \left(\lambda \frac{\partial T}{\partial y} \right) \quad (1)$$

$$\frac{\partial(\rho_{PCM} C_{P\,eff} T_{PCM})}{\partial t} = \frac{\partial}{\partial x} \left(\lambda_{PCM} \frac{\partial T_{PCM}}{\partial x} \right) + \frac{\partial}{\partial y} \left(\lambda_{PCM} \frac{\partial T_{PCM}}{\partial y} \right) \quad (2)$$

$$C_{P\,eff} = \begin{cases} C_{Ps} & \text{for } T < (T_m - \Delta T) \\ \frac{C_{Ps} + C_{Pl}}{2} + \frac{h_{ls}}{2\Delta T} & \text{for } (T_m - \Delta T) < T < (T_m + \Delta T) \\ C_{Pl} & \text{for } T > (T_m + \Delta T) \end{cases}$$

An energy balance was performed at each interface to ensure accurate heat transfer across the roof, which is composed of layers of different materials. This approach guarantees continuity between layers, preventing unwanted heat storage that could distort temperature predictions and affect the evaluation of the roof's thermal performance.

This balance is based on Fourier's Law and is implemented in numerical simulations to model heat transfer accurately through the layers. For these simulations, it is important to have precise and accessible data on the thermal physical properties of the materials involved. Table 1 presents the corresponding properties for each material comprising the roof.

Box 4

Table 1

Thermophysical properties of each layer on the composite roof

| Material | λ , $\text{Wm}^{-1}\text{ }^{\circ}\text{C}^{-1}$ | ρ , kgm^{-3} | C_P , $\text{Jkg}^{-1}\text{ }^{\circ}\text{C}^{-1}$ | h_{ls} , Jkg^{-1} |
|--------------------------|--|-------------------------------|---|---------------------------------|
| Concrete | 1.28 | 2200 | 850 | - |
| Reinforced concrete | 1.74 | 2300 | 920 | - |
| Gypsum plaster | 0.40 | 1200 | 837 | - |
| Polystyrene insulation | 0.03 | 28 | 1800 | - |
| RT25 HC 22°C – 26 °C | 0.20 | 880 770 | 2000 | 230 000 |
| RT35 HC* 29°C – 36 °C | | 860 770 | | 158 000 |
| RT44 HC* 41°C – 44 °C | | 800 700 | | 248 000 |

Source: Own elaboration

The selection of RT25 HC, RT35 HC*, and RT44 HC PCM is based on the ability to optimize the thermal process in accordance with the characteristic temperatures of the local region. The RT25 HC is chosen due to the melting temperature of 25 °C, which matches the desired indoor temperature, allowing it to stabilize this temperature by absorbing excess heat. The RT35 HC*, with a melting temperature close to 35 °C, is selected because it is similar to the sol-air temperature of the region, helping to mitigate daytime heat peaks. Finally, RT44 HC is selected to manage the maximum outdoor temperature, which is close to 44 °C, by absorbing the extreme heat and preventing it from penetrating into the building, thus improving energy efficiency and thermal comfort.

On the other hand, the boundary conditions to solve the mathematical model are expressed by Eq. (3) and (4). Where Eq. (4) takes into account the solar radiation absorbed by the material, the heat transfer by convection with a convective coefficient as a function of the wind velocity, $h_o=2.8+3.0V_{wind}$ (ASHRAE, 2009) and the solar heat transfer towards the sky vault (Swinbank, 1963).

On the lower boundary, similar effects are considered, in this case the convective coefficient varies as a function of the inside surface temperature of the roof, according to Duffie & Beckman (2013), where $h_i=9.26 \text{ Wm}^{-2}\text{K}^{-1}$ if $T_{s,i} < T_i$ and $h_i=6.13 \text{ Wm}^{-2}\text{K}^{-1}$ if $T_{s,i} > T_i$.

$$-\frac{\partial T}{\partial y} = \alpha^* G_{\text{solar}} + h_o(T_{s,o} - T_o) + \varepsilon\sigma(T_{s,o}^4 - T_{\text{sky}}^4) \quad (3)$$

$$-\frac{\partial T}{\partial y} = h_i(T_i - T_{s,i}) + \varepsilon\sigma(T_i^4 - T_{s,i}^4) \quad (4)$$

The model described earlier is two-dimensional, considering that the heat flow occurs mainly in the horizontal and vertical directions, while the lateral surfaces are treated as adiabatic. This assumption allows for a simplified model that maintains the accuracy of the results, as the lateral heat flow is minimal compared to the main flow through the roof. Moreover, even though the correlations for the convection heat transfer coefficients used in this model were developed several decades ago, they remain widely accepted by the scientific community due to their proven effectiveness and reliability in similar applications. These correlations, such as those reported by Duffie and Beckman, have demonstrated reliability across a wide range of weather conditions and continue to serve as a standard reference in heat transfer studies.

To evaluate the thermal performance of the proposed configurations, three key parameters were used: the decrement factor, the time lag, and the thermal load. The decrement factor (DF) measures the roof's capacity to attenuate outside temperature oscillations before they reach the inside, with a low value indicating good thermal attenuation. The time lag (TL) indicates the time taken by the thermal wave to travel through the roof from the outside to the inside surface; for hot climates, a longer time indicates better performance, as it delays the entry of heat into the building. Finally, the thermal load (CT) represents the total amount of heat that must be removed or added to the building to maintain indoor thermal comfort, with a low value indicating good energy efficiency. The thermal load is calculated as the area under the curve that represents both heat gains and losses over time, as shown in Eq. (5).

This calculation reflects the total amount of energy required to maintain a constant indoor temperature within a space, compensating for both heat entering and leaving the system.

$$CT = \int_{00:00}^{24:00} q(t) dt \quad (5)$$

Weather data

For this study, the BWk climate from the Köppen classification was selected, as it is characterized by a cold desert climate with dry winters. This selection is justified by the need to analyze the thermal performance of composite roofs under both high and low extreme temperature conditions typical of regions with this type of climate. In Mexico, this climate is common in cities like Ciudad Juarez, located in the State of Chihuahua, where ambient temperature varies significantly throughout the year.

Ciudad Juarez was selected as the source for the weather data, as it adequately represents the climate spectrum in Mexico, with extreme high and low temperatures typical of the BWk climate. The weather data were obtained from the National Weather System, which provides reliable and accessible information throughout the year. However, due to the high computational resources required for each simulation of every single and double-layer PCM configuration, a decision was made to focus on the most critical days of the year—those with the highest and lowest recorded temperatures. This selection allows for an efficient evaluation of the roof's thermal performance under the most extreme conditions, ensuring that the analyzed configurations can manage both maximum heating and cooling demands.

On the selected days, the outside ambient temperature varied between -7.9°C as the lowest value, and 46.1°C as the highest value (see Figure 4). Throughout the coldest day, the wind velocity varied between 0.0 ms^{-1} and 2.4 ms^{-1} , while on the warmest day, the wind velocity varied between 0.0 ms^{-1} and 4.5 ms^{-1} . For the coldest day, the highest solar irradiance on the horizontal plane was 789 Wm^{-2} , whereas the south-facing vertical plane received the highest solar radiation compared to other orientations.

On the warmest day, the highest solar irradiance was 1028 Wm^{-2} on the horizontal plane, while the west-facing vertical orientation recorded the highest value after midday. Other cities in Mexico with a climate spectrum similar to Ciudad Juarez include Mexicali in Baja California and Hermosillo in Sonora, where ambient temperatures also vary widely, with similar extreme values. These cities, like Ciudad Juarez, experience extremely hot summers and cold winters, making them relevant to this type of study.

Box 5

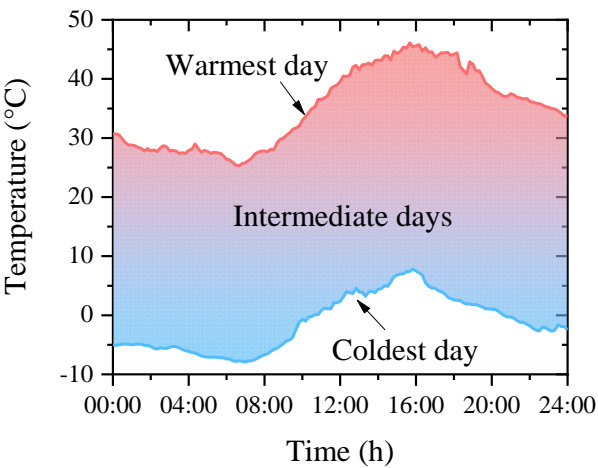


Figure 4
Recorded temperature interval: comparison respect to the climate spectrum of the region
Source: Own elaboration.

Methodology

This study implemented the Finite Volume Method to solve the governing equations for two-dimensional heat conduction in transient states, applicable to both solid materials and phase change materials (PCM). Time discretization employed a fully implicit scheme, and the diffusive term was discretized using a centered scheme. The algebraic equations were solved using the Alternate Directions Gauss-Seidel method (LGS-ADI), with a residual tolerance set at 10^{-8} to ensure accuracy.

The code used in this study is recognized by the scientific community, with some configurations previously published by the authors (López Salazar et al., 2023). To further validate the reliability of the results, the code was additionally tested against experimental data reported by Chagolla-Aranda et al. (2017).

This validation, detailed in Figure 5, demonstrates the code's ability to accurately replicate experimental results, highlighting the robustness and reliability of the implemented numerical code.

Box 6

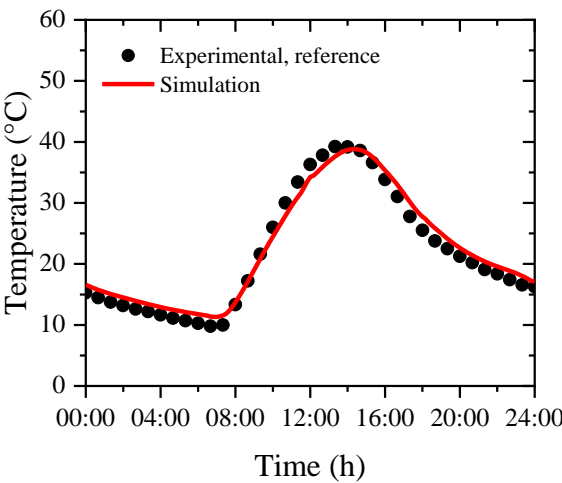


Figure 5
Surface temperature validation of a referenced roof compared to experimental data
Source: Own elaboration

Results

In this section, the results obtained for the different configurations of composite roofs evaluated in this study are presented and analyzed. The configurations include a reference model without additional materials, models with thermal insulation, and those incorporating PCM layers on both the inside and outside surfaces of the reinforced concrete slab. These configurations were designed to assess the thermal performance under extreme weather conditions. The study was divided into three phases to evaluate the impact of different PCM layer thicknesses and combinations:

Phase 1. This phase includes the reference roof, roofs with additional insulation, and roofs with a 10 mm PCM layer on both the outside and inside surfaces. These configurations evaluate how a thinner PCM layer affects thermal attenuation compared to the basic setup.

Phase 2. In this phase, roofs with thicker PCM layers (20 mm and 30 mm) were analyzed to assess how PCM thickness influences thermal storage capacity and indoor temperature regulation.

Phase 3. This phase explored combinations of double PCM layers on both the inside and outside surfaces to determine if combining different types of PCM and their strategic positioning can further optimize heat transfer through the roof.

Table 2 shows the nomenclature used for each case analyzed, to facilitate their identification and allow comparison among the different configurations. The configurations range from the single roof without any additional material to those with thermal insulation and layers of PCM.

Box 7

Table 2
Configuration overview: phases, material composition, and PCM thickness

| Phase 1 |
|--|
| C1. (a) Ref |
| C2. (b) Ref+Ins |
| C3. (c) Ref+e10mmPCMi RT25 HC |
| C4. (c) Ref+e10mmPCMi RT35 HC* |
| C5. (c) Ref+e10mmPCMi RT44 HC |
| C6. (d) Ref+e10mmPCM _o RT25 HC |
| C7. (d) Ref+e10mmPCM _o RT35 HC* |
| C8. (d) Ref+e10mmPCM _o RT44 HC |
| C9. (e) Ref+Ins+e10mmPCMi RT25 HC |
| C10. (e) Ref+Ins+e10mmPCMi RT35 HC* |
| C11. (e) Ref+Ins+e10mmPCMi RT44 HC |
| C12. (f) Ref+Ins+e10mmPCM _o RT25 HC |
| C13. (f) Ref+Ins+e10mmPCM _o RT35 HC* |
| C14. (f) Ref+Ins+e10mmPCM _o RT44 HC |
| Phase 2, 20mm |
| C14-C16, e20 mmPCM |
| Phase 2, 30mm |
| C27 – C38, e30mmPCM |
| Phase 3 |
| C39. (g) Ref+PCMi RT25 HC+PCM _o RT25 HC |
| C40. (g) Ref+PCMi RT25 HC+PCM _o RT35 HC* |
| C41. (g) Ref+PCMi RT25 HC+PCM _o RT44 HC |
| C42. (h) Ref+PCMi RT25 HC+PCM _o RT25 HC |
| C43. (h) Ref+PCMi RT35 HC*+PCM _o RT25 HC |
| C44. (h) Ref+PCMi RT44 HC+PCM _o RT25 HC |
| C45. (i) Ref+DoublePCMi bRT25 HC + tRT35 HC* |
| C46. (i) Ref+DoublePCMi bRT25 HC + tRT44 HC |
| C47. (j) Ref+DoublePCMi bRT35 HC* +tRT25 HC |
| C48. (j) Ref+Double PCMi bRT44 HC + tRT25 HC |
| C40. (i) Ref+DoublePCM _o bRT25 HC + tRT35 HC* |
| C50. (i) Ref+DoublePCM _o bRT25 HC + tRT44 HC |
| C51. (j) Ref+DoublePCM _o bRT35 HC* + tRT25 HC |
| C52. (j) Ref+Double PCM _o bRT44 HC + tRT25 HC |

Source: Own elaboration.

Figure 6 shows the comparison of the thermal performance of the different roof configurations evaluated in this study under the extreme weather conditions recorded on the selected days.

This figure illustrates how each configuration manages heat transfer by comparing the decrement factor (DF), time lag (TL), and thermal load, to identify the configurations that are the most efficient for thermal regulation.

Figure 6a, which corresponds to the coldest day, illustrates how each configuration responds to low outside temperatures. Configurations with PCM on the inside surface, such as C3 and C9, show a lower DF and a longer TL compared to the reference (C1). Notably, configuration C9, which combines insulation with an inside PCM layer, demonstrates a low thermal load, making it an efficient option under cold weather conditions. However, the PCM does not reach the melting point, so no significant phase change is observed.

This indicates that, under these circumstances, the PCM does not actively contribute to heat storage or release, limiting the effectiveness. On the other hand, in configurations belonging to Phase 2, where the PCM thickness was increased to 20 mm and 30 mm (C15 and C38), an additional improvement in thermal attenuation is observed. Configurations with greater PCM thickness are beneficial for reducing heat losses.

Finally, Phase 3 configurations, which evaluate the double PCM layer (C39-C52), exhibit superior thermal performance. Configurations like C39 and C45, which combine different types of PCM on both interior and exterior surfaces, show an extended TL and a low thermal load, proving to be the most effective for maintaining a stable indoor temperature under extremely cold weather.

In contrast, Figure 6b, which corresponds to the warmest day, shows that the PCM undergoes a phase change by absorbing heat when the outside temperatures rise. This demonstrates PCM's ability to regulate heat gain, providing more effective thermal protection. In this high-temperature scenario, configurations C7 and C13, which include PCM on the outside surface, effectively limit heat gain, as seen in the reduced thermal load. In Phase 2, increasing PCM thickness to 20 mm and 30 mm enhances performance under high-temperature conditions.

Configurations such as C28 and C34 show a significant reduction in thermal load, indicating that greater PCM thickness not only reduces heat losses but also limits heat gains on warm days. Phase 3 configurations, which include a double PCM layer, offer the best results. Configurations like C40 and C47 stand out for their ability to extend the time lag and reduce the thermal load, demonstrating their effectiveness in maintaining a comfortable indoor temperature under high-temperature conditions.

Based on the results shown in Figure 6, configuration C45, which incorporates a double layer of PCM with different types of PCM strategically placed on the inside and outside, stands out as the most efficient option for both cold and warm extreme weather conditions. The PCM selection was based on the melting temperature, with materials like RT25 HC for the interior and RT35 HC* for the exterior, allowing phase change across the relevant temperature range for the studied climate. This configuration shows a high capacity to retain indoor heat during the coldest day, due to the low decrement factor and long time lag, while also efficiently limiting heat gains during the warmest daytime and controlling the thermal load. The phase change in the PCM plays a crucial role, as it stores energy as latent heat during warm days and releases it when temperatures drop, something that polystyrene insulation cannot achieve. Due to the versatility and superior performance in both scenarios, configuration C45 emerges as the best option for maintaining thermal comfort and energy efficiency in the building.

Configuration C39, which also has a double layer of PCM, is ranked as the second-best option and offers a good balance between heat conservation and reduction of thermal gains. The third-best option is configuration C9, which combines thermal insulation with a single layer of PCM on the lower surface, standing out primarily for heat conservation during cold days. While the polystyrene acts as a constant barrier against heat transfer, PCM dynamically adapts to varying conditions during phase change, providing greater thermal inertia and improving energy efficiency under extremely fluctuating temperatures.

Configurations in Phase 2, such as C28 and C34, which include thicker layers of PCM (20 mm and 30 mm, respectively), also demonstrate good performance, particularly in reducing thermal loads on warm days. Finally, configurations in Phase 1 like C3 and C7, which use a 10 mm thick PCM, show acceptable performance but are less effective compared to the previously described configurations in attenuating heat loss and limiting thermal gain.

Configuration C2, which incorporates polystyrene insulation, shows moderate performance in thermal attenuation and thermal load management on both the coldest and warmest days. However, configurations that include PCM, such as C45 (double layer of PCM) and C39 (a layer of PCM on the inside and outside surfaces), show better performance under both extreme climate conditions.

On the coldest day, configurations with PCM not only provide better insulation to reduce indoor heat loss but also exhibit a longer time lag and lower thermal load compared to polystyrene. This occurs because, although the PCM does not undergo a phase change during the coldest day, the high thermal storage capacity still contributes to heat conservation. On the warmest day, the PCM also proves to be more efficient at limiting heat gain, offering more effective thermal regulation than polystyrene.

While polystyrene is a widely used and cost-effective insulation material, the results suggest that incorporating PCM instead can significantly enhance the roof's thermal performance, especially in climates with high temperature fluctuations. To optimize energy efficiency and thermal comfort, it is advisable to consider PCM inclusion rather than polystyrene in composite roof applications.

The appropriate hierarchical order to improve the thermal efficiency of the roof begins with adding a PCM layer. Configurations with a PCM layer have shown superior thermal regulation by retaining heat during cold days and effectively limiting heat gain during warm days. The next step is to increase the PCM layer's thickness, providing additional benefits such as increased thermal storage capacity, improved time lag, and further reduced thermal load.

Following this, adding insulation—while having a lesser impact than the PCM layer—remains an effective strategy for enhancing overall thermal efficiency. Finally, adding an extra PCM layer is the most advanced strategy, maximizing thermal efficiency by offering higher storage capacity, though this approach is more complex and expensive to implement. This procedure represents the most effective configuration for optimizing the roof's thermal performance under varying weather conditions.

Box 8

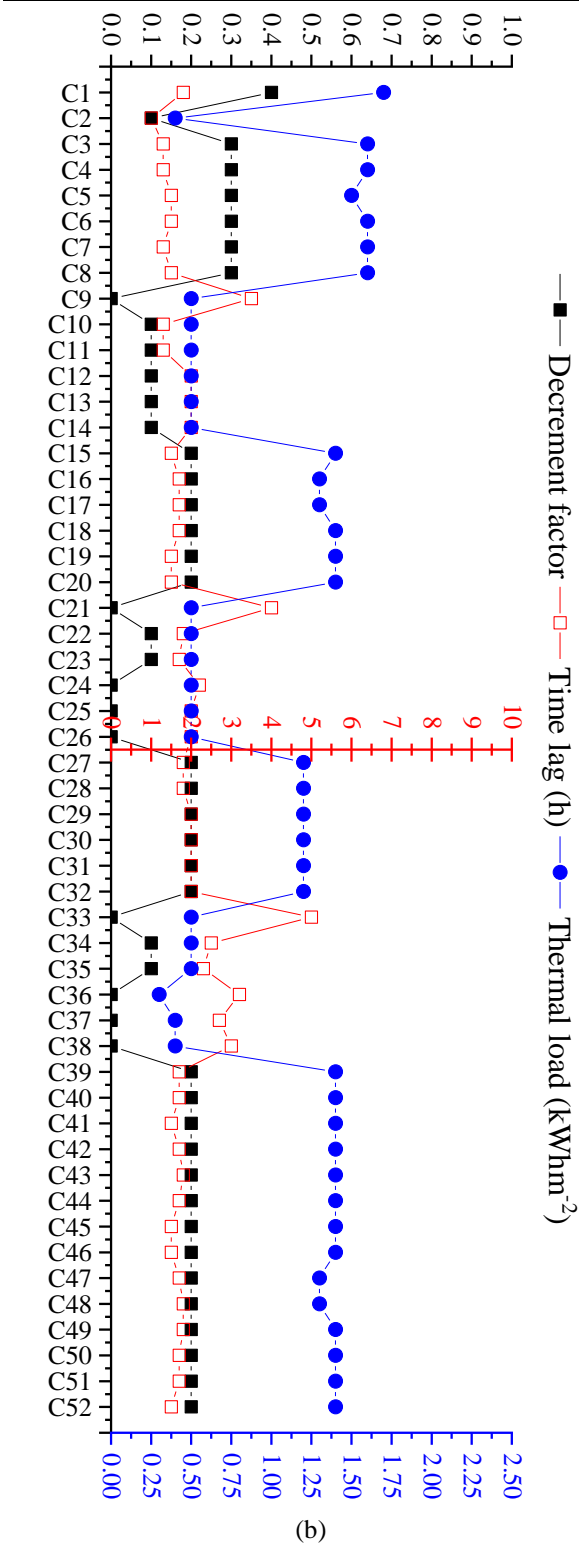
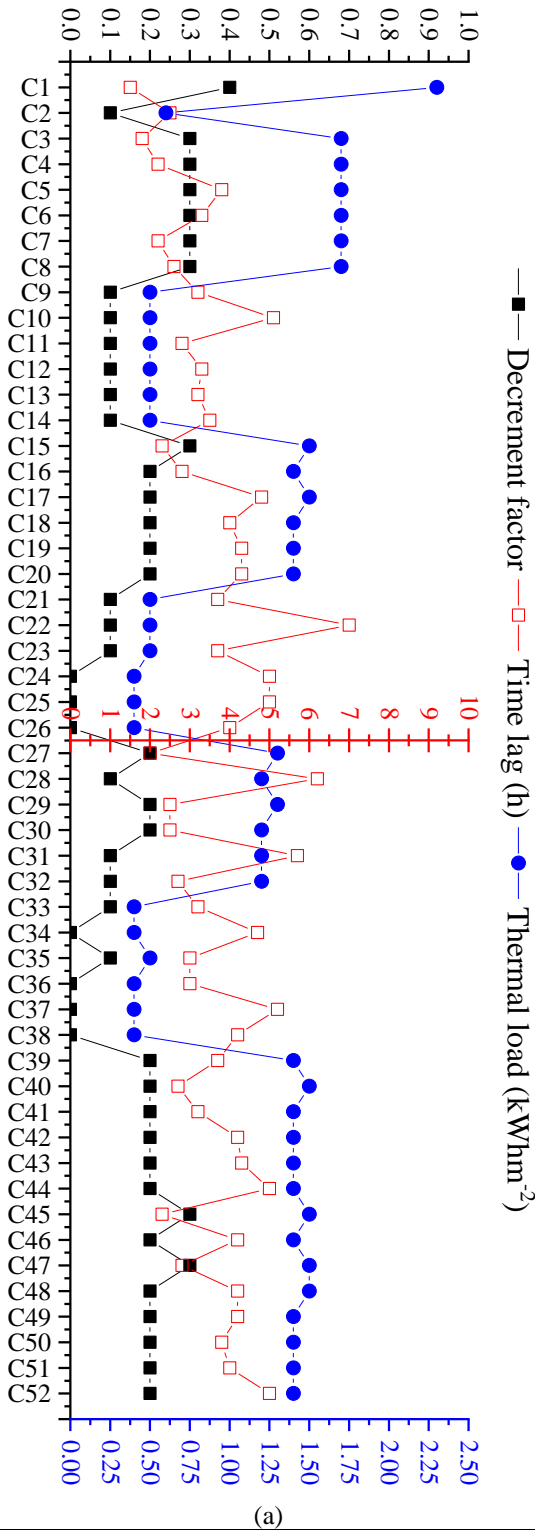


Figure 6
Comparison of the thermal performance on different roofs configurations under extreme weather conditions: (a) coldest day, (b) warmest day

Source: Own elaboration

Therefore, an optimal configuration is one that has a low DF, ideally below 0.2, which indicates an excellent capacity for attenuating outside thermal fluctuations and reducing heat transfer to the interior.

The TL should be appropriate for the weather conditions: a large TL, close to 10 hours, is desirable for warm climates to delay incoming heat, whereas a short TL, around 2-4 hours, is more beneficial for cold climates to allow incoming heat when outside temperatures are low. For thermal load, an efficient configuration should remain below 2.5 kWhm^{-2} , which reflects low energy consumption and a good capacity to maintain a comfortable indoor temperature.

Conclusions

In this study, the thermal performance of different roof configurations was evaluated, focusing on the integration of phase change materials (PCM) compared to traditional thermal insulation methods such as expanded polystyrene. Through numerical analysis, key parameters such as the decrement factor (DF), time lag (TL), and thermal load were analyzed under extreme weather conditions.

The results showed that configurations including a PCM, particularly those with a double layer or thicker PCM, demonstrated significantly better performance. Specifically, the optimal configurations achieved a DF below 0.2, a TL appropriate to the climate (between 2 and 10 hours), and a thermal load lower than 2.5 kWhm^{-2} . Configuration C45, which includes a double layer of PCM with melting temperatures of 25°C and 35°C , located on the inside and outside surfaces respectively, stood out as the most efficient for both the coldest and warmest days, even surpassing configurations with polystyrene insulation.

The comparative and hierarchical analysis of all configurations reveals that the addition of a PCM is the most effective strategy to optimize the thermal performance of roofs, followed by increasing the thickness of the PCM layer, the inclusion of insulation, and finally, the addition of an extra layer of PCM. These strategies progressively improve energy efficiency and indoor thermal comfort.

The comparison with extruded polystyrene showed that, although this material is still an effective and viable option in terms of costs, it does not offer the same level of thermal performance as a PCM, especially under extreme weather conditions.

The phase change capability of a PCM, which enables the material to absorb and release latent heat, is key to the superiority under these conditions, as it significantly improves the thermal inertia of the roof—a behavior that cannot be replicated by polystyrene. Therefore, for applications where thermal efficiency and comfort are to be maximized, the use of a PCM is recommended as an alternative or complement to traditional insulation options.

Finally, this study contributes to the energy efficiency field in construction by providing quantitative data and analysis to guide further investigations and practical applications. The inclusion of PCM in composite roofs not only improves thermal performance but also offers a sustainable solution to reduce energy demand in buildings. Future studies could explore the use of PCM in combination with other advanced materials, as well as extending their application to other types of constructions and weather conditions, thereby widening the possibilities for thermal optimization and energy savings.

Annexes

Declarations

The authors declare that no funds were received to support this research.

Conflict of interest

The authors declare no interest conflict. They have no known competing financial interests or personal relationships that could have appeared to influence the article reported in this article.

Author contribution

López Salazar, Samanta; Conceptualization, Methodology, Software, Writing – original draft preparation.

Simá, E.; Project administration, supervision.

Chagolla-Aranda, M.A.; Formal Analysis, Visualization.

Chávez-Chena, Y.; Writing – review & editing, Formal Analysis.

Availability of data and materials

The data supporting the findings of this study are available from the corresponding author upon reasonable request.

Funding

No funding was received to support this research.

Acknowledgements

López Salazar, Samanta acknowledges the National Council of Humanities, Sciences and Technologies (CONAHCYT) for the financial support given through her doctorate scholarship program (CVU: 918135 and GRANT NUMBER: 789202) as well as the Technological National Institute of Mexico (TecNM-CENIDET).

To Professor J. Xamán †.

Abbreviations

| | |
|---------------|---------------------------------------|
| A | area, m^2 |
| C_p | specific heat, $Jkg^{-1}K^{-1}$ |
| CT | thermal load, $kWhm^{-2}$ |
| DF | decrement factor |
| G | solar radiation, Wm^{-2} |
| q | heat flux per unit area, Wm^{-2} |
| t | time, s |
| T | temperature, $^{\circ}C$ |
| TL | time lag, h |
| α^* | absortance |
| Δt | time step, s |
| ε | emittance |
| λ | thermal conductivity, $Wm^{-1}K^{-1}$ |
| ρ | density, kgm^{-3} |
| ρ^* | reflectance |
| i | indoor environment/inside |
| s, i | inner surface |
| s, o | outdoor surface |
| o | outdoor environment/outside |

References

Antecedents

López Salazar, S., Lima-Téllez, T., Yang, R., Simá, E., Hernandez-López, I., & Dong, L. (2023). [Comparative assessment of roofing strategies for thermal load reduction, energy efficiency, and CO₂ emission mitigation in a tropical climate](#). In P. Moreno-Bernal, P. Escamilla-Ambrosio, L. Hernandez-Callejo, S. Nesmachnow, D. Rossit, & C. Torres-Aguilar (Eds.), VI Ibero-American Congress of Smart Cities (pp. 208-222).

Basics

Somu, N., R, G. R. M., & Ramamritham, K. (2021). [A deep learning framework for building energy consumption forecast](#). *Renewable And Sustainable Energy Reviews*, 137, 110591.

Shove, E., Walker, G., & Brown, S. (2014). [Material culture, room temperature and the social organization of thermal energy](#). *Journal Of Material Culture*, 19(2), 113-124.

Bhamare, D. K., Rathod, M. K., Banerjee, J., & Arıcı, M. (2023). [Investigation of the Effect of Air Layer Thickness on the Thermal Performance of the PCM Integrated Roof](#). *Buildings*, 13(2), 488.

American Society of Heating and Refrigerating and Air-Conditioning Engineers, 680 ASHRAE Handbook of Fundamentals, American Society of Heating and Refrigerating and Air-Conditioning Engineers, Inc., 2009.

Swinbank, W. C. (1963). [Long-wave radiation from clear skies](#). *Quarterly Journal of the Royal Meteorological Society*, 89(381), 339-348.

Duffie, J. A., & Beckman, W. (2013). [Solar engineering of thermal processes](#). En John Wiley & Sons, Inc. eBooks.

Supports

Mejía, K. J., Del Mar Barbero-Barrera, M., & Pérez, M. R. (2020). [Evaluation of the Impact of the Envelope System on Thermal Energy Demand in Hospital Buildings](#). *Buildings*, 10(12), 250.

Wang, H., Chen, Y., Guo, C., Zhou, H., & Yang, L. (2024). [Study on optimal layout and design parameters of ventilated roof for improving building roof thermal performances](#). *Energy and Buildings*, 320, 114576.

Parikh, K., Mehta, S., Gajjar, C., Patel, H., & Patel, G. (2023). [Improving Roof Surface Temperature Control Using Heat-Reflective Inorganic Composition for Paint and Coating Application](#). *Journal Of Testing And Evaluation*, 52(2), 20230377.

Shrimali, R., & Agrawal, N. K. (2024). [Climate responsive insulation strategies: a comparative analysis for enhanced energy conservation and reduced environmental footprint in Indian urban contexts](#). *Environment Development And Sustainability*.

Piselli, C., Castaldo, V. L., & Pisello, A. L. (2019). [How to enhance thermal energy storage effect of PCM in roofs with varying solar reflectance: Experimental and numerical assessment of a new roof system for passive cooling in different climate conditions](#). *Solar Energy*, 192, 106-119.

Bhamare, D. K., Rathod, M. K., & Banerjee, J. (2020). [Numerical model for evaluating thermal performance of residential building roof integrated with inclined phase change material \(PCM\) layer](#). *Journal Of Building Engineering*, 28, 101018.

Arumugam, C., & Shaik, S. (2021). [Air-conditioning cost saving and CO2 emission reduction prospective of buildings designed with PCM integrated blocks and roofs](#). *Sustainable Energy Technologies And Assessments*, 48, 101657.

Qu, Y., Zhou, D., Xue, F., & Cui, L. (2021). [Multi-factor analysis on thermal comfort and energy saving potential for PCM-integrated buildings in summer](#). *Energy And Buildings*, 241, 110966.

Dardouri, S., Tunçbilek, E., Khaldi, O., Arıcı, M., & Sghaier, J. (2023). [Optimizing PCM Integrated Wall and Roof for Energy Saving in Building under Various Climatic Conditions of Mediterranean Region](#). *Buildings*, 13(3), 806.

Dardouri, S., Mankai, S., Almoneef, M. M., Mbarek, M., & Sghaier, J. (2023). [Energy performance based optimization of building envelope containing PCM combined with insulation considering various configurations](#). *Energy Reports*, 10, 895-909.

Dardouri, S., Tunçbilek, E., Khaldi, O., Arıcı, M., & Sghaier, J. (2023). [Optimizing PCM Integrated Wall and Roof for Energy Saving in Building under Various Climatic Conditions of Mediterranean Region](#). *Buildings*, 13(3), 806.

Yu, J., Dong, Y., Zhao, Y., Yu, Y., Chen, Y., & Guo, H. (2023). [Using phase change materials to alleviate overheating phenomenon of residential buildings in severe cold and cold regions of China](#). *Case Studies In Thermal Engineering*, 49, 103207.

Anter, A. G., Sultan, A. A., Hegazi, A., & Bouz, M. E. (2023). [Thermal performance and energy saving using phase change materials \(PCM\) integrated in building walls](#). *Journal Of Energy Storage*, 67, 107568.

Refahi, A., Rostami, A., & Amani, M. (2024). [Implementation of a double layer of PCM integrated into the building exterior walls for reducing annual energy consumption: Effect of PCM wallboards position](#). *Journal Of Energy Storage*, 82, 110556.

Zhang, M., Zheng, Y., He, Y., Jin, Z., Zhang, Y., & Shi, L. (2024). [Novel modular PCM wall board for building heating energy efficiency: Material preparation, manufacture and dynamic thermal testing](#). *Applied Thermal Engineering*, 124168.

Khaleghi, H., & Karatas, A. (2024). [Assessing the dynamic thermal performance of prefabricated wall panels in extreme hot weather conditions](#). *Journal Of Building Engineering*, 82, 108351.

Differences

Arumugam, C., Shaik, S., Roy, A., Kontoleon, K. J., Cuce, E., Shaik, A. H., Chakraborty, S., Alwetaishi, M., Cuce, P. M., & Gupta, M. (2024). [Analysis of the benefits of adopting roof sandwich panels integrated with PCM versus PUR to mitigate energy costs and carbon dioxide emissions](#). *Journal Of Energy Storage*, 77, 109947.

Zahir, M. H., Irshad, K., Shafiullah, M., Ibrahim, N. I., Islam, A. K., Mohaisen, K. O., & Sulaiman, F. A. (2023). [Challenges of the application of PCMs to achieve zero energy buildings under hot weather conditions: A review](#). *Journal Of Energy Storage*, 64, 107156.

Chagolla-Aranda, M., Simá, E., Xamán, J., Álvarez, G., Hernández-Pérez, I., & Téllez-Velázquez, E. (2017). [Effect of irrigation on the experimental thermal performance of a green roof in a semi-warm climate in Mexico](#). *Energy And Buildings*, 154, 232-243.